Fibroblast growth factor 23 regulates hypoxia-induced osteoblast apoptosis through the autophagy-signaling pathway

QIPU YIN[1*], HONGXIA YANG[2*], LUN FANG[1], QI WU[3], SHAN GAO[4], YADI WU[1] and LU ZHOU[1]

[1]Institute of Sports Medicine and [2]School of Nursing, Shandong First Medical University and Shandong Academy of Medical Sciences, Taian, Shandong 271016; [3]Department of Rehabilitation and Physiotherapy, Taian Maternal and Child Health Hospital, Taian, Shandong 271000; [4]School of Pharmaceutical Science, Shandong First Medical University and Shandong Academy of Medical Sciences, Taian, Shandong 271016, P.R. China

Received March 9, 2023; Accepted August 18, 2023

DOI: 10.3892/mmr.2023.13086

Abstract. Hypoxia can lead to programmed osteoblast death. Prevention of osteoblast apoptosis caused by hypoxia is of great significance in the study of the occurrence and development of bone necrosis. The present study aimed to investigate the effects and mechanism of fibroblast growth factor 23 (FGF23) on hypoxia-induced apoptosis in primary osteoblasts and MC3T3-E1 cells osteoblasts. Cells were transfected with a plasmid carrying the FGF23 gene and a cell model of hypoxia-induced apoptosis was established. FGF23 mRNA levels were measured using reverse transcription-quantitative (RT-q) PCR and western blotting was used to assess protein levels. Apoptosis was analyzed by MTT assay, fluorescein diacetate and ethidium bromide staining, flow cytometry and RT-qPCR and western blotting were used to verify the mRNA and protein levels of apoptosis- and autophagy-related gene mRNA. The targeted relationship between miR-17-5p and FGF23 was confirmed using the StarBase database, TargetScan database and a luciferase reporter assay. FGF23 decreased cell survival and increased the rate of apoptosis. The mRNA and protein expression of the pro-apoptotic genes Bax and caspases 3 and 9 increased, whereas that of the anti-apoptotic Bcl-2 decreased. The expressions of the autophagy-associated proteins beclin-1, light chain 3-II (LC3-II) and the LC3-II/LC3-I ratio were significantly increased. In addition, a luciferase reporter assay confirmed that FGF23 directly regulated micro RNA (miR)-17-5p. The effects of FGF23 silencing were reversed by miR-17-5p inhibition. FGF23 may regulate hypoxia-induced osteoblast apoptosis by targeting miR-17-5p through the autophagy-signaling pathway. This provides a rationale for FGF23 as a potential therapeutic target for osteonecrosis of the femoral head.

Correspondence to: Professor Lu Zhou, Institute of Sports Medicine, Shandong First Medical University and Shandong Academy of Medical Sciences, 619 Changcheng Road, Taian, Shandong 271016, P.R. China
E-mail: zhoulu@sdfmu.edu.cn

*Contributed equally

Key words: fibroblast growth factor 23, micro RNA 17-5p, osteoblasts, hypoxia, apoptosis, autophagy

Introduction

Osteonecrosis of the femoral head (ONFH) frequently occurs in young adults and can lead to a high disability rate. The primary mechanism responsible for ONFH development is osteocyte death resulting from damage to microvascular circulation (1). In addition, cell hypoxia due to vascular disruption can give rise to mitochondrial permeability, which may result in apoptosis in smooth muscle, vascular endothelial cells and osteoblasts (2). Furthermore, a number of studies have shown that hypoxia can negatively affect osteoblast proliferation, differentiation and expression of osteoblast-specific genes and proteins (3,4). Therefore, effective prevention of osteoblast apoptosis caused by hypoxia has become a feasible mean for necrosis treatment.

Proteins belonging to the fibroblast growth factor (FGF) family are defined as humoral factors with β-trefoil structures. Humans have at least 22 FGF proteins grouped into several subfamilies (5). FGF1-5 sub-protein molecules are produced in a paracrine form and endocrine-type FGF19, FGF21 and FGF23 regulate activity *in vivo* in a target tissue Klotho protein-dependent manner (6). FGF23 is secreted by osteocytes and osteoblasts and is a phosphophilic hormone that binds to the co-receptor formed by FGFR-αKlotho on the cell membranes of specific tissues and regulates the metabolism of systemic vitamin D and phosphorus (7,8). Phosphorus is one of the major minerals in the body and is involved in bone formation, cell signal transduction, energy metabolism and acid-base balance (9). Studies have reported the regulatory effects of FGF23 on various metabolic and apoptotic processes (10-12). However, the effect of FGF23 on osteoblast apoptosis induced by external injury, especially hypoxia, has not yet been explored.

MicroRNAs (miRNAs/miRs) are a class of non-coding RNAs 18-22 nucleotides in length that repress the expression of target genes post-transcriptionally by complementary pairing with incomplete bases in the bases 3' untranslated

regions, resulting in the translational arrest of target gene mRNAs (13,14). miRNAs are widely involved in developing and progressing various human diseases, including ONFH (15). miR-17-5p, as a member of the miR-17 family, is involved in regulating the progression of osteoarthritis, osteoporosis, ONFH, myocardial ischemia and various tumors (16-20). In addition, studies have shown that miR-17-5p can regulate osteoblast cell differentiation and cell proliferation in non-traumatic ONFH (18,21).

The present study aimed to investigate the role of FGF23 in osteoblasts *in vitro* and the potential mechanisms involved. TargetScan online database predicted miR-17-5p as a target of FGF23. Therefore, it was hypothesized that FGF23 might affect osteoblast apoptosis by targeting miR-17-5p to regulate the autophagy-signaling pathway.

Materials and methods

Cell culture. The MC3T3-E1 osteoblast cell line was obtained from Procell Life Science & Technology Co., Ltd. and the primary osteoblasts were obtained from C57BL/6 mice (22). A total of 12 C57BL/6 mice were used in this study and all animals were housed in the SPF-grade Animal Experiment Center of the Institute of Sports Medicine, Shandong First Medical University, with a room temperature of 22˚C, relative humidity of 55% and 12-h light/dark cycle, standard mice food feeding, free water intake. Chloral hydrate (3%) was used to anesthetize the mice by intraperitoneal injection. Neonatal C57BL/6 mice were sacrificed by cervical dislocation method and disinfected with 70% ethanol and calvaria was predigested in 0.25% trypsin (MilliporeSigma) at 37˚C for 20 min. After the bone fragments were cut into small pieces of ~1 mm^2 and digested in 0.1% collagenase type II (MilliporeSigma) at 37˚C for 50 min to collect the digested product. Digestion of residual bone fragments was repeated once with fresh collagenase. The digested product collected twice was centrifuged at 90 x g at room temperature for 5 min, the supernatant was discarded and the pellet was resuspended and inoculated with Dulbecco's Modified Eagle's Medium (DMEM; Gibco; cat. no. C11995500BT; Thermo Fisher Scientific, Inc.) containing 10% fetal bovine serum (FBS; cat. no. 04-001-1ACS; Biological Industries) and 1% penicillin-streptomycin (MilliporeSigma). The Biomedical Research Ethics Committee of Shandong First Medical University approved this study (Shandong Academy of Medical Sciences; ethics approval no. W202210070243). All cells were cultured in DMEM at 37˚C in a 5% carbon dioxide incubator. The medium was changed two to three times per week.

Transfection. Primary osteoblasts and MC3T3-E1 cells were plated at a density of $1x10^5$ cells/ml in 6-well plates at 37˚C in a 5% CO_2 constant temperature incubator. When the cells were 80% confluent, the plasmids were transfected according to the instructions of the Lipofectamine® 2000 reagent (Invitrogen; Thermo Fisher Scientific, Inc.). The short interfering (si)RNA-FGF23 plasmid (5'-GCTATCACCTACAGATCC ATA-3'), empty vector plasmid (5'-UUCUCCGAACGUGUC ACGU-3'), FGF23 overexpression plasmid (5'-UCCAUGCAG AGGUUAUCUUC-3') and miR-17-5p inhibitor (5'-CAAACA CCUUACACACCAGGUAG-3') were synthesized by Hanbio Biotechnology Co., Ltd. To prepare the transfection mixture, 4 μg of plasmid was added to 500 μl of serum-free medium and 5 μl of Lipofectamine 2000 (cat. no. 11668019; Thermo Fisher) was added to 500 μl of serum-free medium and mixed well and then allowed to stand at room temperature for 20 min. The cells were washed with phosphate-buffered saline (PBS) three times and then 1 ml of Lipofectamine® 2000 transfection mixture and 1.5 ml serum-free medium were added and the cells were incubated for 6 h at room temperature. The cells were then switched to the regular medium and continued to be incubated for 48 h at 37˚C in a 5% carbon dioxide incubator. The transfection efficiency of FGF23 was verified by western blotting. Transfection with an empty vector served as the control for plasmid transfection (23).

Cell model and grouping. The incubators were gassed with nitrogen to maintain an anoxic atmosphere of 5% CO_2 and 95% N_2 (24). The experimental subjects were divided into five groups as follows: Normal control group (NC), hypoxia control group (con), empty vector group (EV), FGF23 overexpression group (FGF23) and FGF23 silencing group (si-FGF23).

MTT assay. Primary osteoblasts and MC3T3-E1 cells were collected from each group, digested with trypsin, plated at $1x10^4$ cells/well in 96-well plates and cultured for 48 h. Three replicate wells were used for each group. Then, 10 μl of 5 mg/ml MTT solution (cat. no. Top0191T; Beijing Biotuoda) were added. After incubation at 37˚C for 4 h, 150 μl dimethyl sulfoxide was added and incubated for 10 min. The absorbance value ($OD_{490\ nm}$) at a wavelength of 490 nm was measured using a microplate reader. Three replicate blank samples were used for testing, three times for each group (25).

Detection of caspase-3 activity. Follow the instructions for using the caspase-3 protein activation assay kit (Nanjing KeyGen Biotech Co., Ltd.), 50 μl of each group of sample proteins were taken, 50 μl 2X reaction buffer and 5 μl caspase-3 substrate were added and then incubated at 37˚C for 4 h in the dark. The absorbance at 405 nm was measured using a microplate reader (2).

Flow cytometry. The influence of hypoxia on apoptosis in the osteoblasts was tested by flow cytometry (FCM; Beckman CytoFLEX FCM; Beckman Coulter) using a phospholipid-binding protein V (Annexin V-FITC)/propidium iodide (PI) kit (US Everbright Inc.). After the experimental hypoxia treatment ended, the cells were washed three times with phosphate buffer, collected by centrifugation at 90 x g at 4˚C for 5 min and resuspended at $5x10^4$ cells/ml in 500 μl binding buffer. The cells were then transferred to Eppendorf tubes and incubated with 5 μl Annexin V-FITC and 5 μl PI for 30 min at room temperature in the dark. Results were analyzed by FlowJo v10.6.2 software. The apoptosis rate is the sum of early apoptosis rate and late apoptosis rate (26).

Fluorescein diacetate (FDA) and ethidium bromide (EB) staining. Transfected cells were seeded in 6-well plates at $1x10^5$ cells/well and washed twice with PBS after 48 h incubation. Then, 100 μl of FDA and EB (MilliporeSigma) were added to each well and incubated at 37˚C in the dark for 10 min before imaging with a fluorescence microscope (27).

Table I. Sequences of primers for reverse transcription-quantitative PCR.

Gene	Sequence, 5'→3'
FGF23	FOR: ATGCTAGGGACCTGCCTTAGA
	REV: GGAGCCAAGCAATGGGGAA
Bax	FOR: AGACAGGGGCCTTTTTGCTAC
	REV: AATTCGCCGGAGACACTCG
Bcl-2	FOR: TGACTTCTCTCGTCGCTACCGT
	REV: CCTGAAGAGTTCCTCCACCACC
caspase-3	FOR: CTCGCTCTGGTACGGATGTG
	REV: TCCCATAAATGACCCCTTCATCA
caspase-9	FOR: GGCTGTTAAACCCCTAGACCA
	REV: TGACGGGTCCAGCTTCACTA
Beclin-1	FOR: GAGATTGGACCAGGAGGAAGCT
	REV: GTGCCAAACTGTCCGCTGTG
Light chain 3	FOR: GGCTACGGCTACTATCGCAC
	REV: GGAGAAGGTTTTGCGGTTGAAA
GAPDH	FOR: AATGGATTTGGACGCATTGGT
	REV: TTTGCACTGGTACGTGTTGAT
U6	FOR: ATGGGTCGAAGTCGTAGCC
	REV: TTCTCGGCGTCTTCTTTCTCG
microRNA 17-5p	FOR: ACACTCCAGCTGGGCAAAGTGCT TACAGTG
	REV: CTCAACTGGTGTCGTGGAGTCGG

FOR, forward; REV, reverse.

Autophagy staining assay. Cellular autophagy was detected with the Cellular Autophagy Staining Assay Kit (cat. no. C3018S; Beyotime Institute of Biotechnology). Monodansylcadaverine (MDC) is an eosinophilic fluorescent probe that can specifically label autophagosomes by ion capture and specific binding to membrane lipids. After the cells were treated accordingly, 1 ml of MDC staining solution was added to each well and incubated for 30 min at 37˚C in a cell incubator protected from light. After washing, 1 ml of Assay Buffer was added and green fluorescence was observed under a fluorescence microscope.

Reverse transcription-quantitative (RT-q) PCR. RT-qPCR was used to assess FGF23 expression. First, total RNA was isolated from primary osteoblasts ($1x10^6$) and MC3T3-E1 cells ($1x10^6$) using an RNA extraction kit (cat. no. BSC52M1; BioFlux) and complementary DNA was synthesized using RT kit (cat. no. BSB07M2B, BioFlux) according to the manufacturer's protocols. The Hieff® qPCR SYBR Green Master Mix (cat. no. 11184ES03; Shanghai Yeasen Biotechnology Co., Ltd.) was used for qPCR. PCR primer sequences are shown in Table I. The prepared cDNA, GAPDH and U6 were used as a template and reference for RT-qPCR reactions. Amplification conditions were as follows: 95˚C for 5 min, 95˚C for 10 sec, 60˚C for 30 sec, 72˚C for 30 sec, for a total of 35 cycles. Finally, the relative FGF23 expression was analyzed using the $2^{-\Delta\Delta Cq}$ method [ΔCq=Cq (target gene)-Cq (reference gene)] (28). Two replicate blank samples were used for each group (29).

Western blotting. Total protein of each group was lysed with RIPA lysis solution (cat. no. R0010; Beijing Solarbio Science & Technology Co., Ltd.). The protein concentration was determined by bicinchoninic acid (BCA; cat. no. PC0020; Beijing Solarbio Science & Technology Co., Ltd.) method. RIPA lysis buffer (Beijing Solarbio Science & Technology Co., Ltd.) was added to extract the total protein fully and ~30 μg per lane of protein samples were resolved by 10% sodium dodecyl sulfate-polyacrylamide gel, after which the proteins were transferred to polyvinylidene (MilliporeSigma) membranes for 1 h at 100 V and blocked for 1 h in 5% skimmed milk powder at room temperature. Primary antibodies against, anti-hypoxia-inducible factor-1α (HIF-1α; 1:1,000; cat. no. 14179; Cell Signaling Technology, Inc.), anti-Bax (1:1,000; cat. no. GB11007; Wuhan Servicebio Technology Co., Ltd.), anti-Bcl-2 (1:1,000; cat. no. sc-492; Santa Cruz Biotechnology, Inc.), anti-caspases-3 (1:1,000; cat. no. sc-7148; Santa Cruz Biotechnology, Inc.) and -9 (1:1,000; cat. no. 9504; Cell Signaling Technology, Inc.), anti-LC3B (1:1,000; cat. no. 3868; Cell Signaling Technology, Inc.), anti-LC3A (1:1,000; cat. no. 4599; Cell Signaling Technology, Inc.) anti-Beclin-1 (1:1,000; cat. no. 3738; Cell Signaling Technology, Inc.) and anti-β-actin (1:1,000; cat. no. GB15001; Wuhan Servicebio Technology Co., Ltd.) were added followed by overnight incubation at 4˚C. After washing with TBST (0.1% Tween 20; cat. no. ST673, Beyotime Institute of Biotechnology), the secondary antibodies, goat anti-mouse IgG (1:2,000; cat. no. GB23301; Wuhan Servicebio Technology Co., Ltd.) and goat anti-rabbit IgG (1:2,000; cat. no. GB23303; Wuhan Servicebio Technology

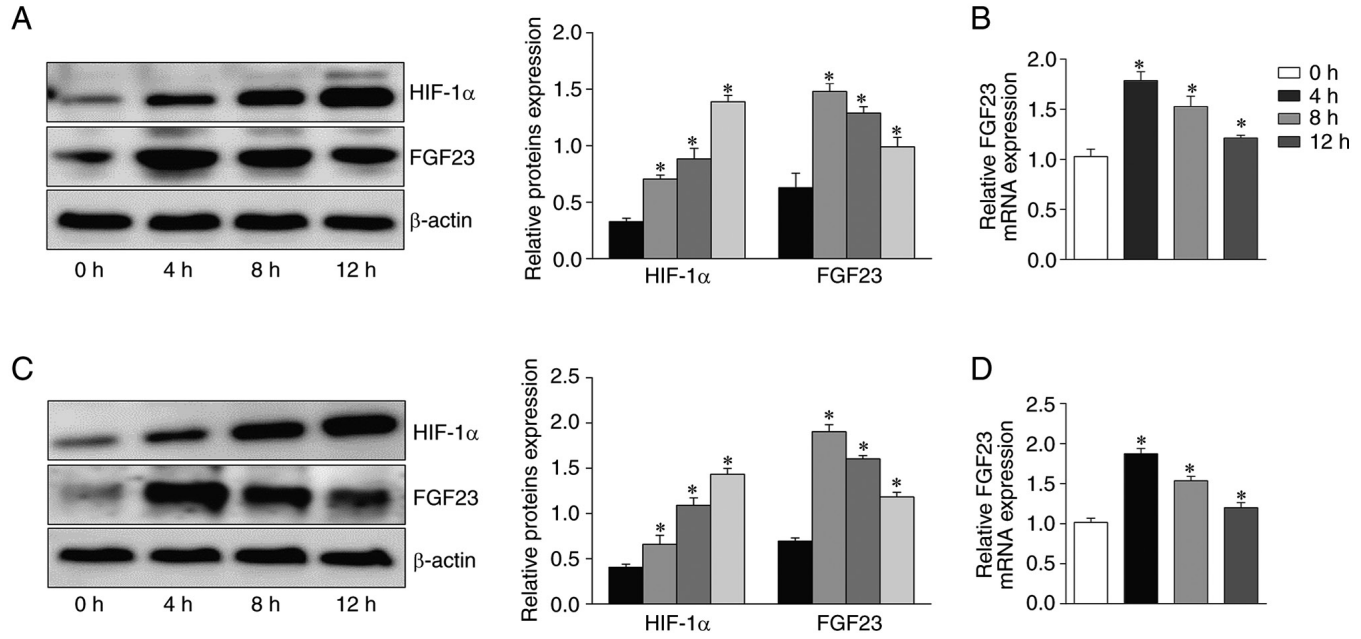

Figure 1. Hypoxia altered FGF23 expression levels in osteoblasts time-dependently. (A) Western blotting and (B) Reverse transcription-quantitative PCR results revealed that FGF23 protein and mRNA expression in MC3T3-E1 cells was the highest in hypoxia for 4 h and then decreased gradually with the extension of hypoxia time. The expression of FGF23 (C) protein and (D) mRNA in primary osteoblasts fluctuated with the change of hypoxia time and the expression was also the greatest at 4 h hypoxia and then gradually decreased. *P<0.05 vs. 0 h. FGF23, fibroblast growth factor; HIF-1α, hypoxia-inducible factor-1α.

Co., Ltd.), were incubated for 1 h at room temperature. Protein bands were visualized using an ECL kit (cat. no. P10200; New Cell & Molecular Biotech Co., Ltd.). The relative expression levels of the proteins were analyzed by ImageJ v1.8.0 software using β-actin as a reference (30).

Dual-luciferase reporter assay. Complementary binding sites between miR-17-5p and FGF23 were predicted using the TargetScan database (http://www.tragetscan.org/) and StarBase database (http://www.starbase.sysu.edu.cn/). Nucleotide sequences containing miR-17-5p binding sites in wild-type (WT) or mutant (MUT) FGF23 3'-UTR were cloned into the pGL3 luciferase reporter plasmid (Invitrogen; Thermo Fisher Scientific, Inc.). MC3T3-E1 cells in the logarithmic growth phase were seeded in 24-well plates ($2x10^5$ cells/well) and the miR-17-5p mimic and miR-NC were co-transfected with WT or MUT reporter plasmids into MC3T3-E1 cells using Lipofectamine® 2000 (Invitrogen; Thermo Fisher Scientific, Inc.) and cultured for 48 h. The fluorescence activity was detected 48 h post-transfection using a dual-luciferase kit (cat.no.E1910; Promega). The firefly and *Renilla* Luciferase activity were detected by the dual luciferase reporter gene detection system and the luciferase activity of the reporter genes was calculated and the luciferase value=Firefly Luciferase activity/*Renilla* Luciferase activity (31).

Statistical analysis. Each experiment was repeated three times. GraphPad Prism v6.02 statistical software (Dotmatics) was used to analyze the data. Normally distributed measurement data are expressed as mean ± standard deviation. The unpaired Student's t test was used for two samples and on way analysis of variance (ANOVA) was used for multiple samples. Tukey's post hoc tests were performed using the Bonferroni method for two samples comparisons between groups. P<0.05 was considered to indicate a statistically significant difference.

Results

The present study verified the hypothesis that FGF23 targets miR-17-5p to regulate hypoxia-induced osteoblast apoptosis by regulating the autophagy-signaling pathway. FGF23 expression was upregulated in osteoblasts following hypoxia treatment. FGF23 overexpression can promote apoptosis and autophagy in osteoblasts. miR-17-5p is a potential biological target of FGF23. It was found that miR-17-5p reversed the biological effects of FGF23. The present study provided a theoretical basis for the clinical treatment and early intervention of ONFH.

Effect of the alteration of hypoxia time on FGF23 expression level in osteoblasts. The levels of FGF23 in the cells after apoptosis induction under different hypoxic conditions were evaluated by western blotting and RT-qPCR. Due to alterations in hypoxia time, the expression levels of FGF23 protein and mRNA in osteoblasts showed significant fluctuations. Western blotting showed that FGF23 protein expression was the highest at 4 h and then gradually decreased with the extension of hypoxia time in in MC3T3-E1 cells (P<0.05; Fig. 1A). The RT-qPCR results were consistent with the western blotting results (Fig. 1B). Additionally, HIF-1α expression increased under prolonged hypoxia for up to 12 h (Fig. 1A). FGF23 protein and mRNA expression in primary osteoblasts was highest at 4 h and then gradually decreased (Fig. 1C and D). These results indicated that the expression

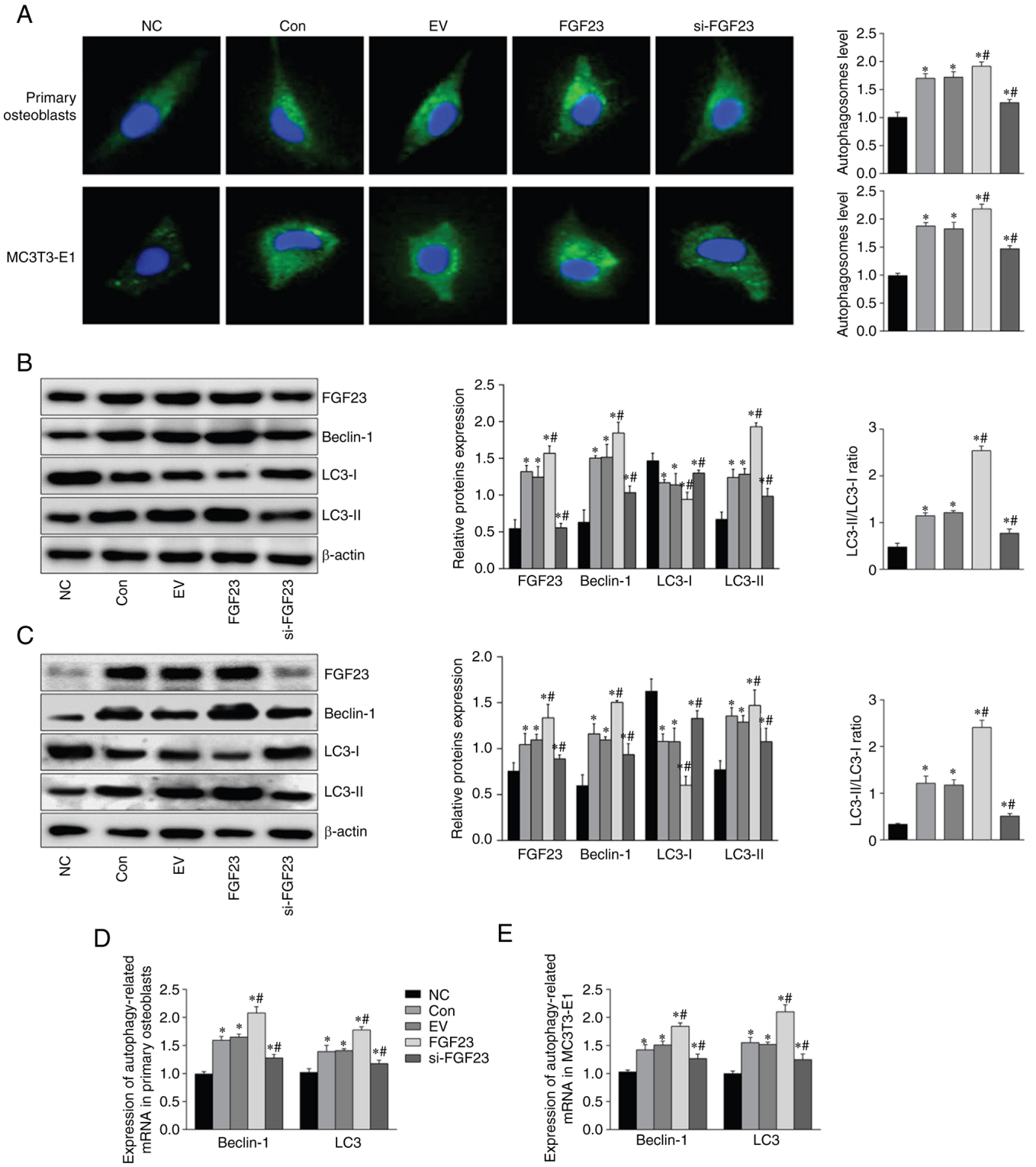

Figure 2. FGF23 promotes hypoxia-induced autophagy in osteoblasts. (A) Detection of intracellular autophagosomes by Monodansylcadaveriner staining (magnification, x400). The expression of FGF23, Beclin-1, LC3-I and LC3-II in (B) primary osteoblasts and (C) MC3T3-E1 cells was detected via western blotting. The mRNA level of Beclin-1 and LC3 of (D) primary osteoblasts and (E) MC3T3-E1 cells. B-actin and GAPDH expression were used to determine the target protein's expression or gene. *P<0.05 vs. NC group. #P<0.05 vs. EV group. Among them, the FGF23 group had the lowest cell survival rate. FGF23, fibroblast growth factor; LC3, light chain 3; NC, normal control; con, control; EV, empty vector group; si, short interfering.

of FGF23 is influenced by hypoxic environments and associated with time. Therefore, hypoxia for 4 h was selected for the following experiments. MC3T3-E1 cells, a mouse osteogenic precursor cell line, are commonly used to study ONFH (32,33).

Effects of hypoxia and FGF23 on autophagy-associated gene and protein expression in primary osteoblasts and MC3T3-E1 cells. Increased autophagosomes were found in primary osteoblasts and MC3T3-E1 cells following hypoxia, and FGF23 knockdown partially reversed this result (Fig. 2A). Western

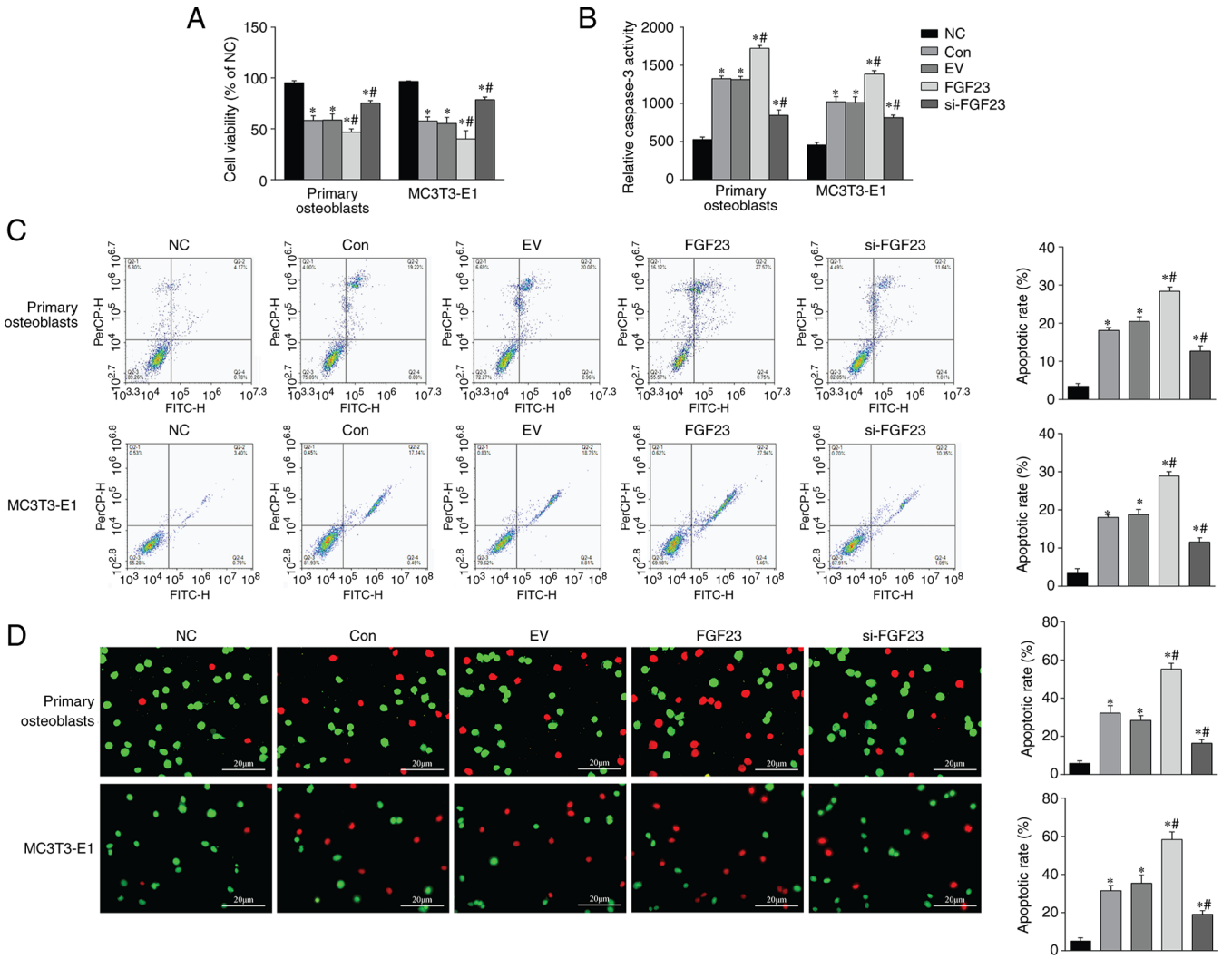

Figure 3. FGF23 promotes hypoxia-induced apoptosis in osteoblasts. (A) The MTT assay shows the effects of various interfering factors on cell survival. (B) Effect of FGF23 on caspase-3 enzyme activity in osteoblasts using caspase-3 protein activation assay kit. (C) Flow cytometry shows the influence of FGF23 on cell apoptosis of hypoxia-induced osteoblasts. (D) Fluorescein diacetate and ethidium bromide staining showed that green fluorescence and red fluorescence presented as viable and dead cells with normal structures, respectively. All the data showed that cell survival was decreased in the experimental groups. *P<0.05 vs. NC. #P<0.05 vs. EV group. FGF23, fibroblast growth factor; NC, normal control, con, control; EV, empty vector group; si, short interfering.

blotting demonstrated that the protein levels of FGF23 were altered by transfection (Fig. 2B and D). Significant increases were observed in the levels of microtubule-associated protein light chain-phosphatidylethanolamine conjugate (LC3-II), Beclin-1 and LC3-II/LC3-I ratio, under hypoxic conditions (P<0.05). Furthermore, compared with the EV group, Beclin-1, LC3-II and the LC3-II/LC3-I ratio were increased in the FGF23 group; however, they were significantly decreased in the si-FGF23 group (Fig. 2B and D). In addition, autophagy-related gene expression also showed corresponding alterations (Fig. 2C and E). Taken together, these results indicate that FGF23 can promote hypoxia-induced autophagy levels in osteoblasts.

Increased FGF23 exacerbates hypoxic apoptosis of osteoblasts. MTT assay was used to measure the influence of different factors on cell viability. The viability was reduced in the con, FGF23 overexpression and si-FGF23 groups compared with the NC group. The FGF23 overexpression group had the lowest cell survival rate (P<0.05; Fig. 3A). FGF23 could significantly increase activity of caspase-3 compared with that in the EV group (P<0.05; Fig. 3B). FCM and FDA/EB staining showed increased apoptosis of osteoblasts in the EV group. However, the FGF23 group showed significantly increased apoptosis compared with the EV group, whereas apoptosis decreased slightly in the si-FGF23 group (Fig. 3C-D). These results indicated that FGF23 might activate the apoptosis pathway and promote cell death during hypoxic cellular stress.

Expression of apoptosis-associated genes and proteins in hypoxic primary osteoblasts and MC3T3-E1 cells. Western blotting results showed that hypoxia led to a significant increase in levels of pro-apoptotic proteins Bax, caspases-3 and -9 and a decrease in levels of anti-apoptotic protein Bcl-2 in primary osteoblasts and MC3T3-E1 cells. Western blotting results showed significantly increased levels of the pro-apoptotic proteins Bax and caspases-3 and -9 and decreased levels of anti-apoptotic Bcl-2 (Fig. 4A and C). The RT-qPCR data showed enhanced expression of the pro-apoptotic (Bax and caspases-3 and -9) mRNA. By contrast, the apoptosis suppressor Bcl-2 mRNA was diminished in osteoblasts compared with the NC group in

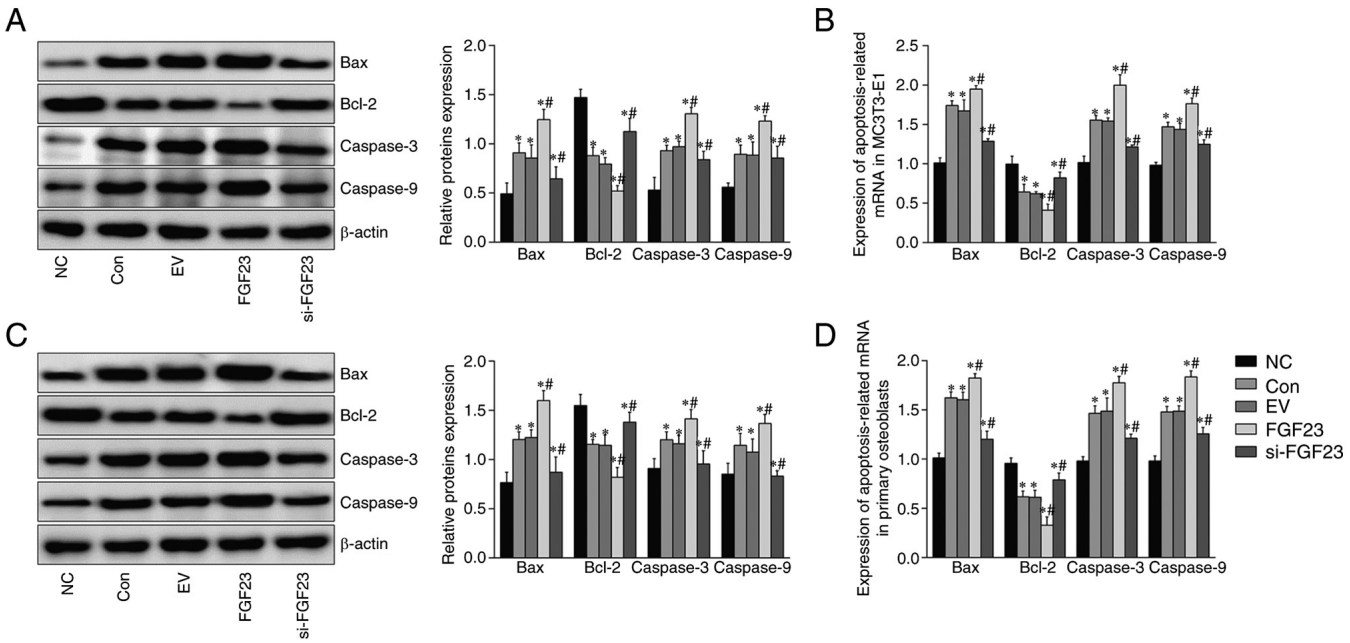

Figure 4. Interference of FGF23 on hypoxia-induced osteoblasts apoptosis. (A) Bax, Bcl-2, caspase-3 and caspase-9 protein levels in primary osteoblasts. (B) Expression of apoptosis-related genes in primary osteoblasts. (C) Expression levels of apoptosis-related proteins in MC3T3-E1 cells. (D) Expression levels of apoptosis-related genes in MC3T3-E1 cells. The relative expression of the target protein and genes was measured with the expression of β-actin and GAPDH separately. *P<0.05 vs. NC group. #P<0.05 vs. EV group. FGF23, fibroblast growth factor; NC, normal control; con, control; si, short interfering.

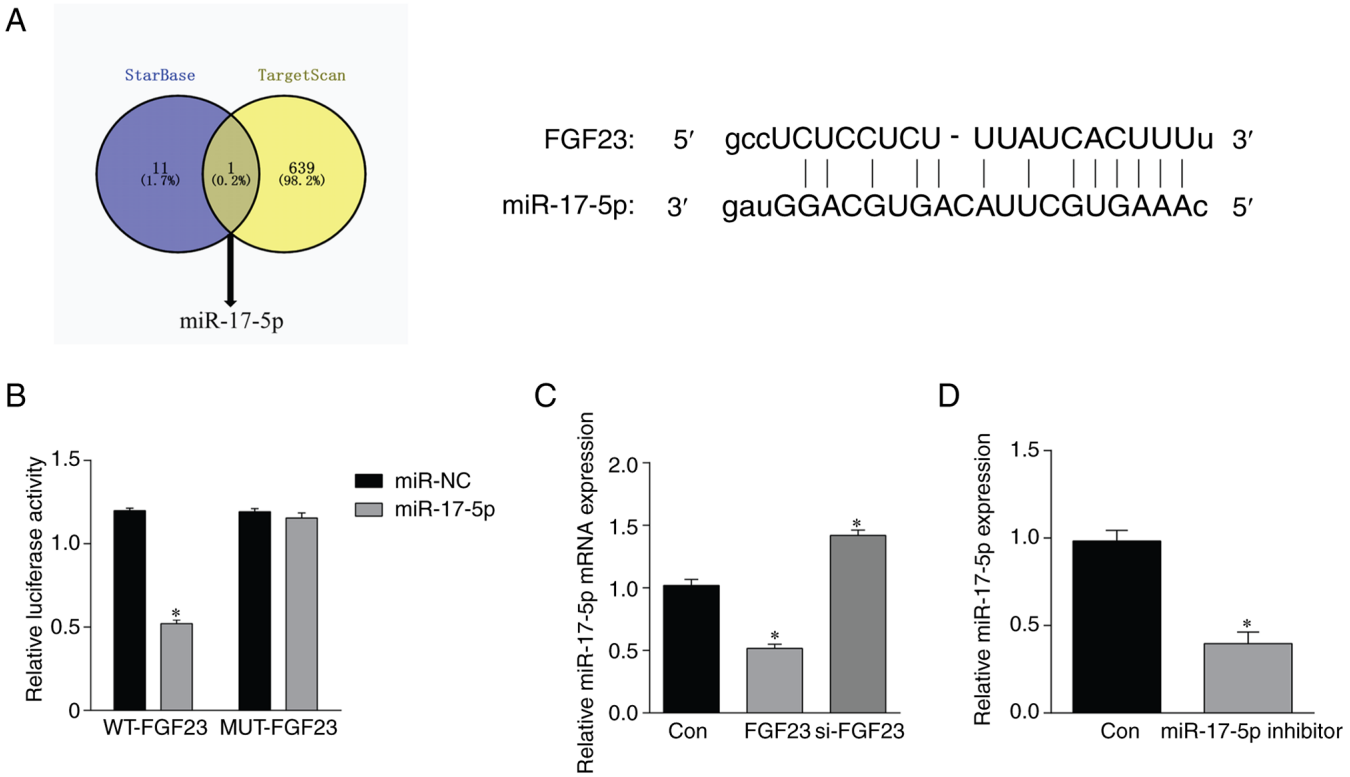

Figure 5. FGF23 targets miR-17-5p. (A) Potential binding sites exist between FGF23 and miR-17-5p by the online database TargetScan and StarBase. (B) miR-17-5p inhibited the luciferase activity of wild-type FGF23; however, it had no significant effect on MUT FGF23. (C) mRNA level of miR-17-5p was decreased after overexpression of FGF23 and increased after silencing FGF23, measured with the expression of U6. (D) Transfection efficiency of miR-17-5p inhibitor. *P<0.05 vs. NC group. FGF23, fibroblast growth factor; miR, microRNA; MUT, mutant; WT, wild type; NC, normal control; con, control; si, short interfering.

response to FGF23. The differences were statistically significant (Fig. 4B and D). Apoptosis levels were further elevated following FGF23 overexpression, whereas, FGF23 knockdown attenuated the apoptosis level in osteoblasts compared with the con group. The above results indicated that knockdown of FGF23 can ameliorate hypoxia-induced apoptosis in osteoblasts.

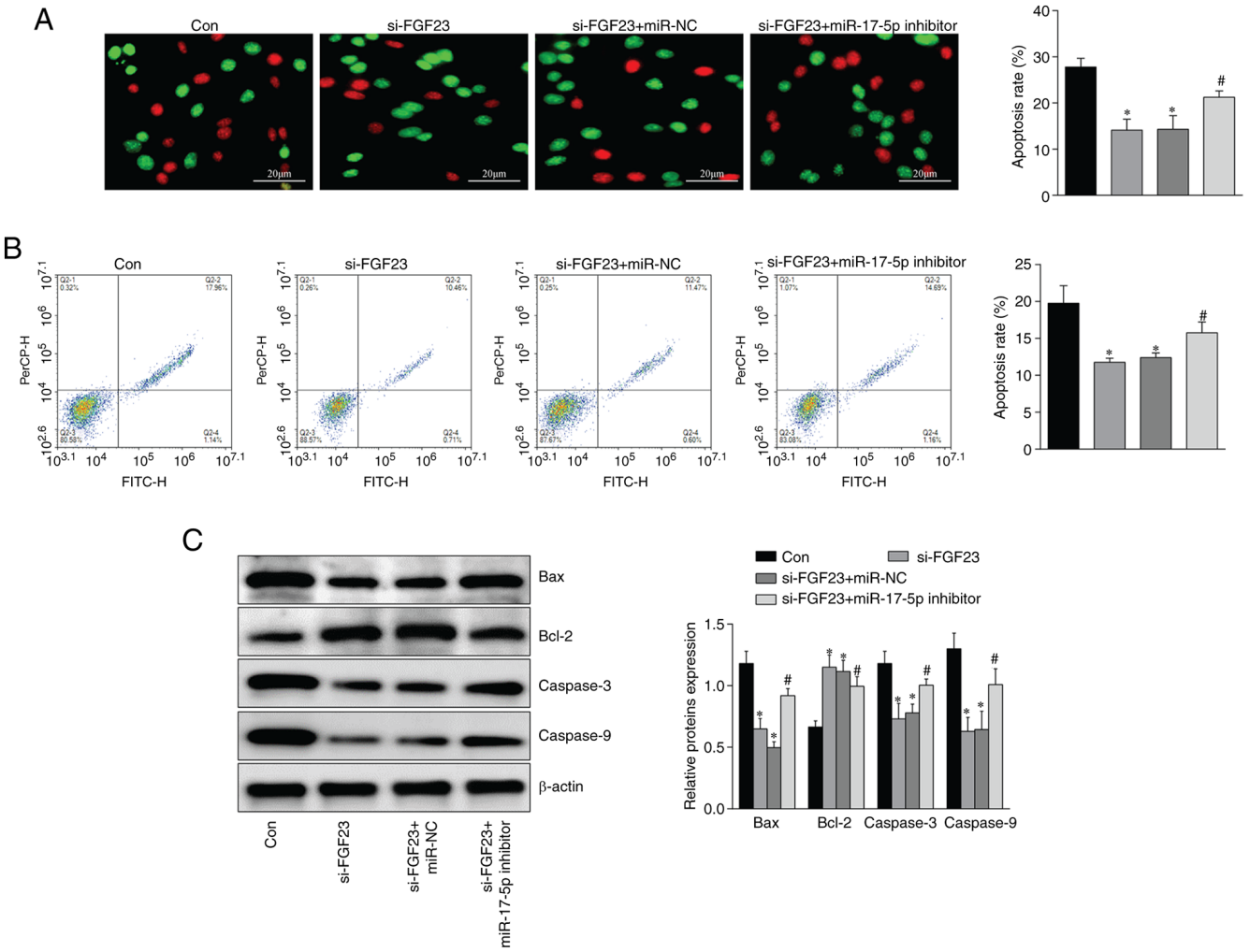

Figure 6. Effect of FGF23 on MC3T3-E1 cells was restored by miR-17-5p inhibitor. The results of (A) Fluorescein diacetate and ethidium bromide staining and (B) Flow cytometry showed the effect of miR-17-5p on the viability of MC3T3-E1 cells after silencing FGF23. (C) miR-17-5p inhibitor elevated the effect of silencing FGF23 on expression of apoptosis-related proteins. *P<0.05 vs. con group. #P<0.05 vs. si-FGF23 + miR-NC group. FGF23, fibroblast growth factor; miR, microRNA; NC, normal control; con, control; si, short interfering.

FGF23 targets miR-17-5p. To further investigate the molecular mechanisms by which FGF23 regulates osteoblast apoptosis, a potential binding site between FGF23 and miR-17-5p was identified by the online database TargetScan and StarBase (Fig. 5A). Subsequent overexpression or inhibition of miR-17-5p was performed for dual luciferase reporter gene assay. As shown in Fig. 5B, luciferase analysis revealed that the FGF23 wild-type luciferase activity in the miR-17-5p group was lower than that in the miR-NC group (P<0.05). By contrast, there was no statistically significant difference in the FGF23 MUT luciferase activity between the miR-17-5p and miR-NC groups (P>0.05). In addition, RT-qPCR results showed that the expression level of miR-17-5p was downregulated after overexpression of FGF23; it was significantly upregulated after the silencing of FGF23 (Fig. 5C). Detection of cell transfection efficiency revealed that transfection with miR-17-5p inhibitor downregulated miR-17-5p expression (Fig. 5D).

Inhibition of miR-17-5p reverses the effect of silencing FGF23 on apoptosis of MC3T3-E1 cells. Compared with the con group, the apoptosis rate (Fig. 6A and B), Bax, caspase-3 and caspase-9 protein (Fig. 6C) expression were significantly decreased, and Bcl-2 protein expression was increased, in MC3T3-E1 cells in the si-FGF23 group. Conversely, compared with the si-FGF23 group, Bax, caspase-3 and caspase-9 protein expression and apoptosis rate were significantly increased. Bcl-2 expression was downregulated in MC3T3-E1 cells in the si-FGF23 + miR-17-5p inhibitor group (Fig. 6).

FGF23 activates the autophagy signaling pathway via targeted regulation of miR-17-5p. FGF23 knockdown reduced the number of autophagosomes, which was partly reversed by the addition of miR-17-5p inhibitor (Fig. 7A). The expression of the autophagy-associated proteins Beclin-1 and LC3 was detected by western blotting and RT-qPCR. The results showed that Beclin-1 and LC3-II/LC3-I expression decreased after FGF23 silencing, whereas this result was partially reversed after miR-17-5p inhibition (Fig. 7B and C).

Discussion

The present study found that hypoxia led to apoptosis and increased FGF23 expression in osteoblasts, whereas FGF23

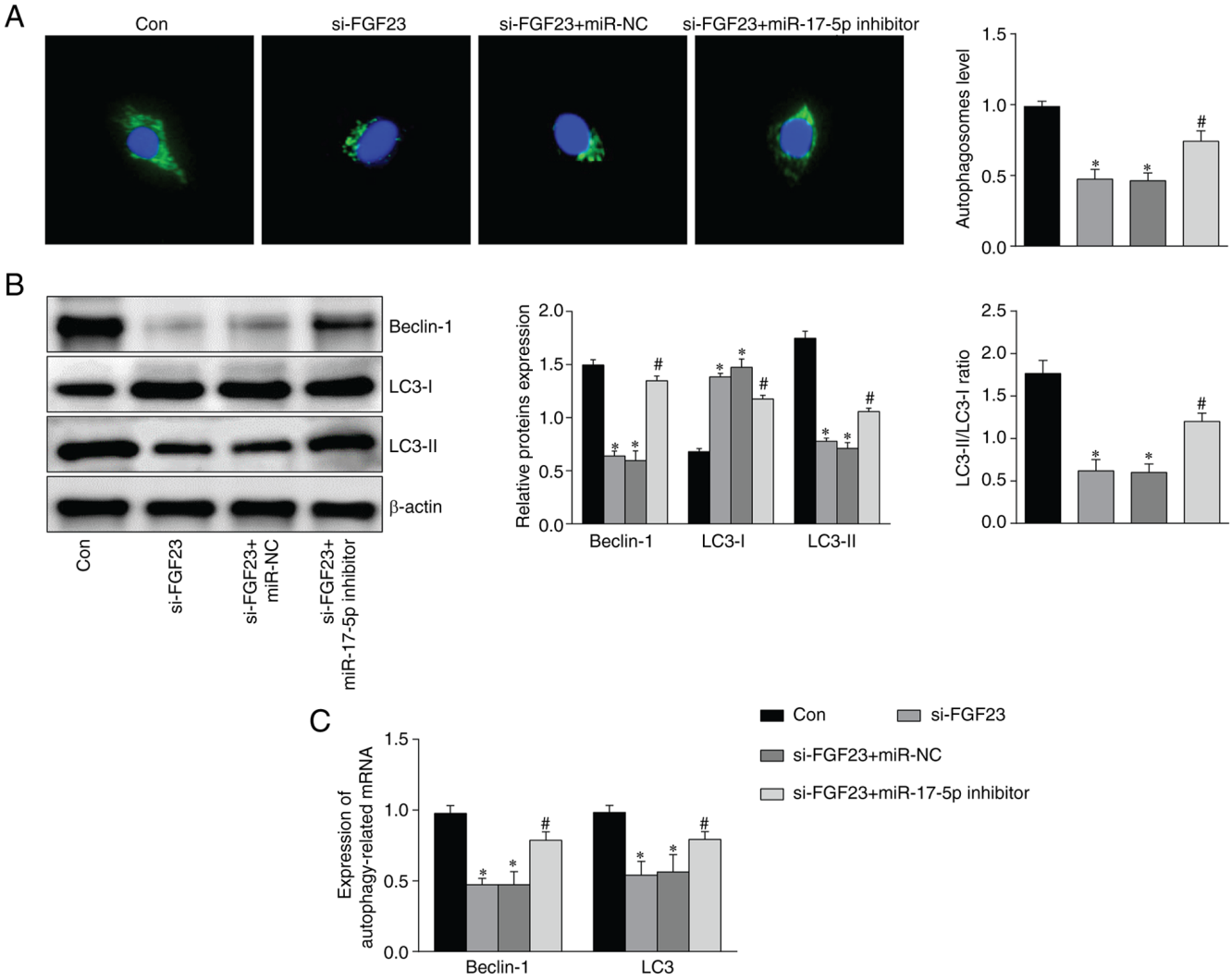

Figure 7. FGF23 activates the autophagy-signaling pathway by targeting and regulating miR-17-5p. (A) Detection of intracellular autophagosomes by Monodansylcadaveriner staining (magnification, x400). (B) The expression of autophagy-related proteins after transfection with si-FGF23 and miR-17-5p inhibitor. (C) Silencing-FGF23 increased the level of autophagy in MC3T3-E1 cells when transfected with the miR-17-5p inhibitor as detected by reverse transcription-quantitative PCR. *P<0.05 vs. con group. #P<0.05 vs. si-FGF23 + miR-NC. FGF23, fibroblast growth factor; miR, microRNA; NC, normal control; con, control; si, short interfering; LC3, light chain 3.

overexpression further aggravated osteoblast apoptosis. To the best of the authors' knowledge, the present study is the first to demonstrate that FGF23 regulates hypoxia-induced apoptosis of osteoblasts by regulating the activation of the autophagy-signaling pathway.

FGF is the most widely distributed growth factor *in vivo*. FGF family members are involved in numerous cellular functions, including metabolic and transcriptional regulation (34). FGF23 modulates cellular energy metabolism and apoptosis. The present study observed that hypoxia increased LC3-II and Beclin-1 in MC3T3-E1 osteoblasts, whereas FGF23 treatment further increased LC3-II and Beclin-1 expression. The microtubule-associated protein light chain 3 (LC3) is an autophagy-related gene expressed in the initial stages of autophagosome formation, promoting autophagy; LC3-I to LC3-II conversion is necessary for completing the process (35). Beclin-1 is a specific autophagy-related gene and its expression level directly reflects autophagic activity (36). The present study indicated that the autophagic activity of MC3T3-E1 osteoblasts was induced in a hypoxic environment and was enhanced in response to FGF23. It has been demonstrated that osteoblast apoptosis and autophagy occur in the early stage of avascular ONFH and that the protein and mRNA expression of LC3B and caspase-3 are significantly upregulated. By contrast, inhibition of autophagy can protect osteoblasts from apoptosis (37,38). Zheng *et al* (39) reported that the hypoxic microenvironment activates autophagy in periodontal ligament tissue, inhibits osteogenic differentiation and promotes apoptosis. Therefore, apoptosis has an intricate relationship with autophagy (40). Normally, autophagy occurs at low levels; however, when cells are stimulated by hypoxia, hormones, or other factors, the process is activated, resulting in the breakdown of the damaged material into small molecules that can participate in energy metabolism (41,42). However, excessive autophagy can potentially affect metabolism and cause cell death (43).

To further validate the function of FGF23 in the apoptosis pathway, hypoxia-induced expression of apoptosis-associated proteins in osteoblasts was assessed.

Caspase-3 activity assay indicated that FGF23 was involved in hypoxia-induced apoptosis. Caspase family proteases are core proteases that mediate apoptosis and can induce apoptosis in a cascading manner, directly leading to cell disassembly. Caspase-9 initiates the apoptotic program, whereas caspase-3 executes it (44-46). In the present study, western blotting results showed that MC3T3-E1 cells treated with FGF23 overexpression showed increased expression levels of the pro-apoptotic proteins caspases-3 and -9 and Bax and decreased expression levels of the anti-apoptotic protein Bcl-2. This result was reversed following intervention with FGF23 silencing. Bcl-2 stabilizes mitochondria, blocks the release of calcium ions from the endoplasmic reticulum, regulates the transduction of mitochondrial signaling molecules, interrupts DNA apoptosis and protects cells from apoptotic damage (47). When cells receive signaling stimuli such as death, Bax translocates from the cytoplasm into the mitochondria and interacts with the anti-apoptotic factor Bcl-2 on the mitochondrial membrane; thus, the anti-apoptotic factor is inactivated, the release of pro-apoptotic factors is increased, the mitochondrial structure and function are destroyed and, finally, the caspase pathway is activated to initiate apoptosis (48). Therefore, Bcl-2 and Bax are essential for cell survival and death (49). In the present study, MTT results revealed that FGF23 led to a decrease in MC3T3-E1 cell viability. Concurrently, FGF23 promoted hypoxia-induced osteoblast apoptosis directly by FC and FDA/EB staining. In addition, in osteoarthritis, FGF23 can regulate 1,25-dihydroxyvitamin D3 and extracellular inorganic phosphate, which significantly upregulates caspase-9 expression and increases apoptosis in normal chondrocytes (50).

Using the TargetScan database, the binding of miR-17-5p and FGF23 was predicted. A luciferase reporter assay confirmed that miR-17-5p is a target of FGF23. miR-17-5p overexpression decreased the luciferase activity of WT-FGF23 but had no effect on MUT-FGF23. Furthermore, it has been shown that miR-17-5p plays an important role in cell proliferation, differentiation and apoptosis (51,52). miR-17-5p regulates osteoblast differentiation and cell proliferation by inhibiting SMAD7 in non-traumatic ONFH (18). In addition, miR-17-5p inhibits chondrocyte apoptosis by targeting enhancer of zeste homolog 2, inhibiting osteoarthritis progression (16). Therefore, the present study investigated whether miR-17-5p inhibitor is a direct target after discovering that it can regulate osteoblast apoptosis. This conjecture was confirmed by FDA/EB staining, FCM and western blotting, suggesting that the miR-17-5p inhibitor partly reversed the effect of FGF23 silencing on osteoblast apoptosis. According to previous studies, miR-17-5p may be involved in the autophagy signaling pathway (53,54). Therefore, it was hypothesized that FGF23 might regulate the autophagy signaling pathway by targeting miR-17-5p. The results showed that FGF23 silencing significantly decreased the expression of Beclin-1 protein and the LC3-II/LC3-I ratio, whereas miR-17-5p had the opposite effect on the expression of these proteins after inhibition. The results showed that FGF23 could affect osteoblast apoptosis by targeting miR-17-5p via the autophagy signaling pathway.

The present study demonstrated that FGF23 regulates hypoxia-induced osteoblast apoptosis by targeting miR-17-5p through the autophagy-signaling pathway. The findings provided foundational support for the clinical prevention and treatment of orthopedic diseases, such as ONFH, caused by various injuries. However, only *in vitro* tests were performed in the present study, which were not able to simulate the *in vivo* state.

Acknowledgements

Not applicable.

Funding

The present study was supported by Shandong Provincial Natural Science Foundation of China (grant no. ZR2019MH120) and the Projects of Medical and Health Technology Development Program in Shandong Province (grant no. 2019WS397).

Availability of data and materials

The datasets generated and analyzed during the present study are available from the corresponding author on reasonable request.

Authors' contributions

QY, HY and LZ designed the study and performed the experiments, LF and QW collected the data, SG and YW analyzed the data and QY and HY prepared the manuscript. QY and LZ confirm the authenticity of all the raw data. All authors read and approved the final manuscript.

Ethics approval and consent to participate

The present study was approved by the Research Ethics Committee of Shandong First Medical University (Shandong Academy of Medical Sciences; grant no. W202210070243).

Patient consent for publication

Not applicable.

Competing interests

The authors declare that they have no competing interests.

References

1. Cohen-Rosenblum A and Cui Q: Osteonecrosis of the femoral head. Orthop Clin North Am 50: 139-149, 2019.
2. Zhou L, Wang SI, Moon YJ, Kim KM, Lee KB, Park BH, Jang KY and Kim JR: Overexpression of SIRT1 prevents hypoxia-induced apoptosis in osteoblast cells. Mol Med Rep 16: 2969-2975, 2017.
3. Wang G, Wang J, Sun D, Xin J, Wang L, Huang D, Wu W and Xian CJ: Short-term hypoxia accelerates bone loss in ovariectomized rats by suppressing osteoblastogenesis but enhancing osteoclastogenesis. Med Sci Monit 22: 2962-2971, 2016.
4. Ma HP, Ma XN, Ge BF, Zhen P, Zhou J, Gao YH, Xian CJ and Chen KM: Icariin attenuates hypoxia-induced oxidative stress and apoptosis in osteoblasts and preserves their osteogenic differentiation potential in vitro. Cell Prolif 47: 527-539, 2014.

5. Itoh N and Ornitz DM: Evolution of the Fgf and Fgfr gene families. Trends Genet 20: 563-569, 2004.
6. Gohil A and Imel EA: FGF23 and associated disorders of phosphate wasting. Pediatr Endocrinol Rev 17: 17-34, 2019.
7. Chen G, Liu Y, Goetz R, Fu L, Jayaraman S, Hu MC, Moe OW, Liang G, Li X and Mohammadi M: α-Klotho is a non-enzymatic molecular scaffold for FGF23 hormone signalling. Nature 553: 461-466, 2018.
8. Andrukhova O, Zeitz U, Goetz R, Mohammadi M, Lanske B and Erben RG: FGF23 acts directly on renal proximal tubules to induce phosphaturia through activation of the ERK1/2-SGK1 signaling pathway. Bone 51: 621-628, 2012.
9. Prié D, Forand A, Francoz C, Elie C, Cohen I, Courbebaisse M, Eladari D, Lebrec D, Durand F and Friedlander G: Plasma fibroblast growth factor 23 concentration is increased and predicts mortality in patients on the liver-transplant waiting list. PLoS One 8: e66182, 2013.
10. Fukumoto S: FGF23 and bone and mineral metabolism. Handb Exp Pharmacol 262: 281-308, 2020.
11. Millar SA, Anderson SI and O'Sullivan SE: Osteokines and the vasculature: A review of the in vitro effects of osteocalcin, fibroblast growth factor-23 and lipocalin-2. PeerJ 7: e7139, 2019.
12. Domazetovic V, Falsetti I, Ciuffi S, Iantomasi T, Marcucci G, Vincenzini MT and Brandi ML: Effect of oxidative stress-induced apoptosis on active FGF23 levels in MLO-Y4 cells: The protective role of 17-β-estradiol. Int J Mol Sci 23: 2103, 2022.
13. Ramzan F, Vickers MH and Mithen RF: Epigenetics, microRNA and metabolic syndrome: A comprehensive review. Int J Mol Sci 22: 5047, 2021.
14. Wen J, Huang Y, Li H, Zhang X, Cheng P, Deng D, Peng Z, Luo J, Zhao W, Lai Y and Liu Z: Over-expression of miR-196b-5p is significantly associated with the progression of myelodysplastic syndrome. Int J Hematol 105: 777-783, 2017.
15. Liu GZ, Chen C, Kong N, Tian R, Li YY, Li Z, Wang KZ and Yang P: Identification of potential miRNA biomarkers for traumatic osteonecrosis of femoral head. J Cell Physiol 235: 8129-8140, 2020.
16. Li Y, Yuan F, Song Y and Guan X: miR-17-5p and miR-19b-3p prevent osteoarthritis progression by targeting EZH2. Exp Ther Med 20: 1653-1663, 2020.
17. Su Y, Meng X, Wang W, Gu G and Chen Y: LncRNA HOTAIR regulates fracture healing in osteoporotic rats through inhibition on MiR-17-5p. Minerva Med 112: 525-527, 2021.
18. Jia J, Feng X, Xu W, Yang S, Zhang Q, Liu X, Feng Y and Dai Z: MiR-17-5p modulates osteoblastic differentiation and cell proliferation by targeting SMAD7 in non-traumatic osteonecrosis. Exp Mol Med 46: e107, 2014.
19. Hou W, Song L, Zhao Y, Liu Q and Zhang S: Inhibition of beclin-1-mediated autophagy by MicroRNA-17-5p enhanced the radiosensitivity of glioma cells. Oncol Res 25: 43-53, 2017.
20. Chen B, Yang Y, Wu J, Song J and Lu J: microRNA-17-5p down-regulation inhibits autophagy and myocardial remodelling after myocardial infarction by targeting STAT3. Autoimmunity 55: 43-51, 2022.
21. Fang T, Wu Q, Zhou L, Mu S and Fu Q: miR-106b-5p and miR-17-5p suppress osteogenic differentiation by targeting Smad5 and inhibit bone formation. Exp Cell Res 347: 74-82, 2016.
22. Hou Z, Wang Z, Tao Y, Bai J, Yu B, Shen J, Sun H, Xiao L, Xu Y, Zhou J, *et al*: KLF2 regulates osteoblast differentiation by targeting of Runx2. Lab Invest 99: 271-280, 2019.
23. Huang X, Chen C, Chen Y, Xu J and Liu L: Omentin-1 alleviate interleukin-1β(IL-1β)-induced nucleus pulposus cells senescence. Bioengineered 13: 13849-13859, 2022.
24. Liu X, Bian H, Dou QL, Huang XW, Tao WY, Liu WH, Li N and Zhang WW: Ginkgetin alleviates inflammation, oxidative stress, and apoptosis induced by hypoxia/reoxygenation in h9c2 cells via caspase-3 dependent pathway. Biomed Res Int 2020: 1928410, 2020.
25. Wang W, Zhu M, Xu Z, Li W, Dong X, Chen Y, Lin B and Li M: Ropivacaine promotes apoptosis of hepatocellular carcinoma cells through damaging mitochondria and activating caspase-3 activity. Biol Res 52: 36, 2019.
26. Xiong H, Li Y and Liu M: DEPDC1B is involved in the proliferation, metastasis, cell cycle arrest and apoptosis of colon cancer cells by regulating NUP37. Mol Med Rep 27: 126, 2023.
27. Qi J, Cao F, Han Y, Xie D, Song H, Chen B and Zhou L: Reliability of cartilage digestion and FDA-EB fluorescence staining for the detection of chondrocyte viability in osteochondral grafts. Cell Tissue Bank 19: 399-404, 2018.
28. Livak KJ and Schmittgen TD: Analysis of relative gene expression data using real-time quantitative PCR and the 2(-Delta Delta C(T)) method. Methods 25: 402-408, 2001.
29. Yi WR, Tu MJ, Yu AX, Lin J and Yu AM: Bioengineered miR-34a modulates mitochondrial inner membrane protein 17 like 2 (MPV17L2) expression toward the control of cancer cell mitochondrial functions. Bioengineered 13: 12489-12503, 2022.
30. Pang X, Wang SS, Zhang M, Jiang J, Fan HY, Wu JS, Wang HF, Liang XH and Tang YL: OSCC cell-secreted exosomal CMTM6 induced M2-like macrophages polarization via ERK1/2 signaling pathway. Cancer Immunol Immunother 70: 1015-1029, 2021.
31. Song J, Liu Y, Wang T, Li B and Zhang S: MiR-17-5p promotes cellular proliferation and invasiveness by targeting RUNX3 in gastric cancer. Biomed Pharmacother 128: 110246, 2020.
32. Lu P, Shen YM, Hua T, Pan T, Chen G, Dai T and Shi KQ: Overexpression of FGF2 delays the progression of osteonecrosis of the femoral head activating the PI3K/Akt signaling pathway. J Orthop Surg Res 16: 613, 2021.
33. Bai Y, Liu Y, Jin S, Su K, Zhang H and Ma S: Expression of microRNA-27a in a rat model of osteonecrosis of the femoral head and its association with TGF-β/Smad7 signalling in osteoblasts. Int J Mol Med 43: 850-860, 2019.
34. Savchenko E, Teku GN, Boza-Serrano A, Russ K, Berns M, Deierborg T, Lamas NJ, Wichterle H, Rothstein J, Henderson CE, *et al*: FGF family members differentially regulate maturation and proliferation of stem cell-derived astrocytes. Sci Rep 9: 9610, 2019.
35. Mancias JD and Kimmelman AC: Mechanisms of selective autophagy in normal physiology and cancer. J Mol Biol 428: 1659-1680, 2016.
36. Musumeci G, Castrogiovanni P, Trovato FM, Weinberg AM, Al-Wasiyah MK, Alqahtani MH and Mobasheri A: Biomarkers of chondrocyte apoptosis and autophagy in osteoarthritis. Int J Mol Sci 16: 20560-20575, 2015.
37. Zheng L, Wang W, Ni J, Mao X, Song D, Liu T, Wei J and Zhou H: Role of autophagy in tumor necrosis factor-α-induced apoptosis of osteoblast cells. J Investig Med 65: 1014-1020, 2017.
38. Zheng LW, Wang WC, Mao XZ, Luo YH, Tong ZY and Li D: TNF-α regulates the early development of avascular necrosis of the femoral head by mediating osteoblast autophagy and apoptosis via the p38 MAPK/NF-κB signaling pathway. Cell Biol Int 44: 1881-1889, 2020.
39. Zheng J, Zhu X, He Y, Hou S, Liu T, Zhi K, Hou T and Gao L: CircCDK8 regulates osteogenic differentiation and apoptosis of PDLSCs by inducing ER stress/autophagy during hypoxia. Ann N Y Acad Sci 1485: 56-70, 2021.
40. Zhang T, Li Y, Park KA, Byun HS, Won M, Jeon J, Lee Y, Seok JH, Choi SW, Lee SH, *et al*: Cucurbitacin induces autophagy through mitochondrial ROS production which counteracts to limit caspase-dependent apoptosis. Autophagy 8: 559-576, 2012.
41. Ho TT, Warr MR, Adelman ER, Lansinger OM, Flach J, Verovskaya EV, Figueroa ME and Passegué E: Autophagy maintains the metabolism and function of young and old stem cells. Nature 543: 205-210, 2017.
42. Manai F, Azzalin A, Gabriele F, Martinelli C, Morandi M, Biggiogera M, Bozzola M and Comincini S: The in vitro effects of enzymatic digested gliadin on the functionality of the autophagy process. Int J Mol Sci 19: 635, 2018.
43. Wang Z, Xie Q, Zhou H, Zhang M, Shen J and Ju D: Amino acid degrading enzymes and autophagy in cancer therapy. Front Pharmacol 11: 582587, 2021.
44. Shi Y: Apoptosome: The cellular engine for the activation of caspase-9. Structure 10: 285-288, 2002.
45. Fan TJ, Han LH, Cong RS and Liang J: Caspase family proteases and apoptosis. Acta Biochim Biophys Sin (Shanghai) 37: 719-727, 2005.
46. Araya LE, Soni IV, Hardy JA and Julien O: Deorphanizing caspase-3 and caspase-9 substrates in and out of apoptosis with deep substrate profiling. ACS Chem Biol 16: 2280-2296, 2021.
47. Perini GF, Ribeiro GN, Pinto Neto JV, Campos LT and Hamerschlak N: BCL-2 as therapeutic target for hematological malignancies. J Hematol Oncol 11: 65, 2018.
48. Ly JD, Grubb DR and Lawen A: The mitochondrial membrane potential (deltapsi(m)) in apoptosis; an update. Apoptosis 8: 115-128, 2003.

49. Shu Y, Yang Y, Zhao Y, Ma L, Fu P, Wei T and Zhang L: Melittin inducing the apoptosis of renal tubule epithelial cells through upregulation of Bax/Bcl-2 expression and activation of TNF-α signaling pathway. Biomed Res Int 2019: 9450368, 2019.
50. Orfanidou T, Malizos KN, Varitimidis S and Tsezou A: 1,25-Dihydroxyvitamin D(3) and extracellular inorganic phosphate activate mitogen-activated protein kinase pathway through fibroblast growth factor 23 contributing to hypertrophy and mineralization in osteoarthritic chondrocytes. Exp Biol Med (Maywood) 237: 241-253, 2012.
51. Shi YP, Liu GL, Li S and Liu XL: miR-17-5p knockdown inhibits proliferation, autophagy and promotes apoptosis in thyroid cancer via targeting PTEN. Neoplasma 67: 249-258, 2020.
52. Li H, Li T, Wang S, Wei J, Fan J, Li J, Han Q, Liao L, Shao C and Zhao RC: miR-17-5p and miR-106a are involved in the balance between osteogenic and adipogenic differentiation of adipose-derived mesenchymal stem cells. Stem Cell Res 10: 313-324, 2013.
53. Hao MX, Wang X and Jiao KL: MicroRNA-17-5p mediates hypoxia-induced autophagy and inhibits apoptosis by targeting signal transducer and activator of transcription 3 in vascular smooth muscle cells. Exp Ther Med 13: 935-941, 2017.
54. Yuan Y, Li X and Li M: Overexpression of miR-17-5p protects against high glucose-induced endothelial cell injury by targeting E2F1-mediated suppression of autophagy and promotion of apoptosis. Int J Mol Med 42: 1559-1568, 2018.